Virtual Connectivity Is a Mixed Blessing for Ride-Hail

Kenan Zhang†[1], Hongyu Chen†[1], Song Yao[2], Linli Xu[2], Jiaoju Ge[3], Xiaobo Liu[4], and Yu (Marco) Nie *[1]

[1]Department of Civil and Environmental Engineering, Northwestern University, IL 60208
[2]Carlson School of Management, University of Minnesota, MN 55455
[3]Harbin Institute of Technology Shenzhen Graduate School, Shenzhen, China
[4]School of Transportation and Logistics, Southwest Jiaotong University, Chengdu, China

Thanks to *virtual connectivity* enabled by internet and mobile computing, activities that once depended on physical interactions can now be accomplished at one's fingertips. In ride-hail, it has created Transportation Network Companies (TNC) such as Uber and Lyft, which offer the *e-hail* service to match passengers with drivers through their smart phones. In this research, by analyzing hundreds of local ride-hail markets in Shenzhen, China for one week, we show that e-hail is often outperformed by its antiquated competitors - taxis hailed off street (*s-hail*) - in areas with high density of passengers and drivers. We further explain this counterintuitive finding using a general theory of the ride-hail matching mechanism. It reveals that virtual connectivity helps e-hail improve matching efficiency by expanding passengers' access to vacant vehicles. However, the matching mechanism acts against e-hail as the market scales up with more passengers and drivers, because virtual connectivity induces congestion among waiting passengers competing for the same pool of vacant vehicles. The finding has implications for the future of urban mobility, as e-hail is often seen as a key ingredient in the forthcoming era of mobility-as-a-service[1,2]. In particular, it implies that (*i*) e-hail's appeal as a mass transporter warrants scrutiny because it scales worse than taxis; and (*ii*) a larger TNC holds no advantage of scale over a smaller competitor. Moreover, the mechanism identified herein, through which virtual connectivity falls victim to its own success, may find applications in other domains.

E-hail is praised for lowering waiting time while serving more trips, because it matches passengers and drivers more efficiently than s-hail[3,4]. Surprisingly, few studies have validated this claim with empirical evidence, even though ride-hail has been studied extensively[5–9]. Motivated by the question, we analyzed s-hail and e-hail operational data collected in the city of Shenzhen, China, for a full week in 2016. For each day of the week, the data are aggregated for two three-hour periods and 277 local markets located in six municipal districts of the city (see [S2] in SI and Fig. E4 in Extended Data). Fig. 1 examines system output (pickup rate m), supply (vacant vehicle density Λ), and average waiting time (AWT $\bar{w}$) at the district level. The supply consists of both committed (Λ_1) and uncommitted (Λ_0) vacant vehicles. The former refers to those en route to pick up passengers and the latter refers to those waiting to be matched. Hence, for e-hail, $\Lambda = \Lambda_0 + \Lambda_1$, and for s-hail, $\Lambda = \Lambda_0$. The result shows that e-hail produces more pickups than s-hail in districts with a relatively low density of passengers and drivers (e.g., suburbs S-1 and S-2), but falls behind in high-density downtown districts (i.e., D-1 and D-2). What is most surprising is not that e-hail produces fewer pickups in downtown areas, but that it

*Corresponding author, E-mail: y-nie@northwestern.edu.
†These authors contributed equally to the work.

does so with longer average waiting and more vacant-vehicle supply. Also note that the majority of the e-hail vacant vehicles in D-1 and D-2 is committed supply (Λ_1), indicating picking up passengers is a serious burden in these areas.

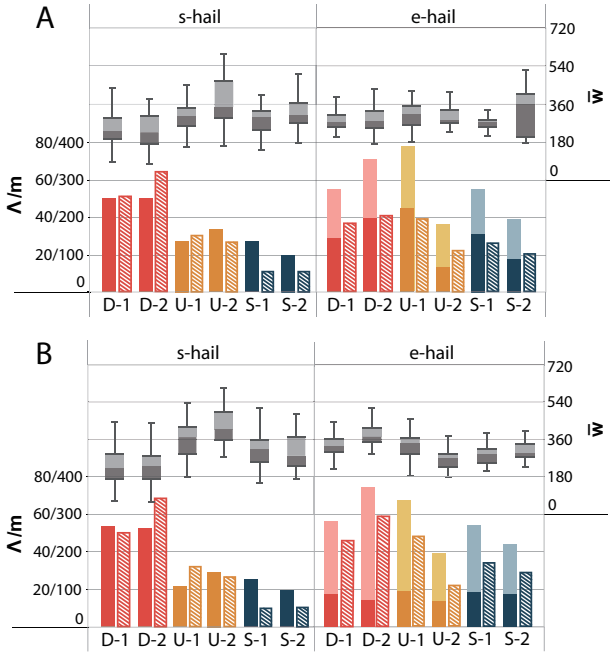

Figure 1: Aggregate service performance of s-hail and e-hail by municipal districts. (**A**) Morning off-peak period (9:00-12:00). (**B**) Evening peak period (17:00-20:00). The districts are classified as downtown (D-1 and D-2), urban (U-1 and U-2), and suburban (S-1 and S-2), see Fig. E4 in Extended Data. The solid bar represents average vacant vehicles per km^2 (Λ). For e-hail, the light (dark) colored portion corresponds to committed (uncommitted) vehicles Λ_1 (Λ_0). The bar with diagonal lines represents hourly pickup rate (m). AWT ($\bar{w}$, sec.) is presented as box plots, where the box represents the 1st and 3rd quantiles and whiskers denote the highest/lowest datum within 1.5 IQR (i.e., the difference between the 1st and 3rd quantiles). For e-hail, the passenger waiting time is computed as the time elapsed from the order placement to the driver's arrival. For s-hail, the passenger waiting time is not directly observed but inferred based on calibrated models (see *Methods*).

To examine e-hail's underperformance, we further explore the relationships between AWT, Λ_0, and m at the local market level. Figs. 2 (A) and (C) show that (*i*) an increase in uncommitted supply reduces AWT for both s-hail and e-hail, and (*ii*) e-hail reduces the likelihood of long waits. Specifically, about 88% of e-hail markets have a 90 percentile waiting time shorter than 10 minutes, compared to 40% for s-hail (see Fig. E1 in Extended Data). Although these findings are expected, it is less clear why AWT of s-hail decreases more sharply than that of e-hail as uncommitted supply increases. Fig. 2 (B) reveals AWT of s-hail decreases with the pickup rate. In other words, the service gets better as more people use it. This seemingly counterintuitive phenomenon is known as the Mohring effect, widely observed in mass-transit systems[10]. The Mohring effect states that an increase in demand may shorten passenger waiting time as it drives up service frequency. However, e-hail demonstrates an almost opposite trend in this relationship: As the pickup rate grows, AWT becomes slightly longer (Fig. 2(D)). This unexpected finding suggests a counter force takes away the Mohring effect from e-hail.

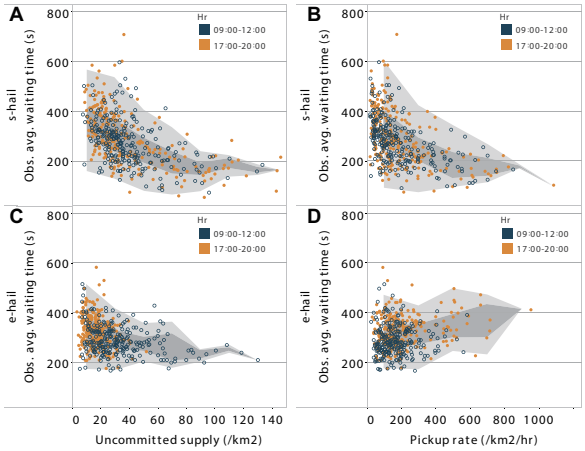

Figure 2: Relationship between AWT, uncommitted-vehicle density and pickup rate. Each data point represents one local market at a given time period. The darker gray area is drawn with 1st and 3rd quantiles of datum aggregated at an interval of 20/km2 for uncommitted supply and 200/km2/hr for the pickup rate. The lighter gray area represents the same aggregated data within 1.5 IQR.

The Mohring effect implies mass-transit systems display increasing returns to scale; that is, output increases more than the proportional change in all inputs[10]. This property has been repeatedly invoked to justify subsidizing public transportation[6;11;12]. The absence of the ef-

fect from e-hail, therefore, signals a potential decline in its returns to scale. To test this hypothesis, we adopt the Cobb-Douglas production function[13]

$$m = \beta \Lambda^{\alpha} \Pi^{\alpha}, \tag{1}$$

where m is the hourly pickup rate; Λ is the density of vacant vehicles ($veh./km^2$); Π is the density of waiting passengers ($pas./km^2$); β is the total factor productivity (TFP), interpreted as the pickup rate when $\Lambda = \Pi = 1/km^2$; and α is the output elasticity to Π and Λ, assumed to be identical for simplicity. The standard economic theory states that the production displays constant/increasing/decreasing returns to scale when 2α is equal to/greater than/less than 1. We fit the linear equation $\log(m) = \log\beta + \alpha[\log(\Pi) + \log(\Lambda)]$ with empirical data for both e-hail and s-hail. The regression result indicates e-hail is about 15 times more efficient than s-hail, measured by the TFP (β). It also shows e-hail displays close-to-constant returns to scale, whereas s-hail shows strong increasing returns to scale (see Fig. 3).

Therefore, empirical evidence does not support e-hail as an unequivocal winner. With better connectivity, e-hail mitigates passengers' exposure to long waits, and significantly raises the industry's factor productivity (β), especially in low-density areas. However, that very advantage turns out to be a mixed blessing, substantially reducing e-hail's returns to scale and compromising its competitive advantage in high-density areas. In the following, we explain this seemingly surprising finding, using a general physical model of ride-hail matching mechanism.

The model is driven by the notion of *reachable vacant vehicles* (hence called the ReV model hereafter), which may be viewed as the share of supply allocated to a passenger entering the market (see Fig. 4). It has two key parameters that must be calibrated to fit a given local market: (*i*) *Effective Hailing Distance* (EHD, or d) specifies the maximum distance from which a vacant vehicle can be hailed by the passenger; it defines a circular *EHD area* centered at the passenger's waiting location, with a radius d;

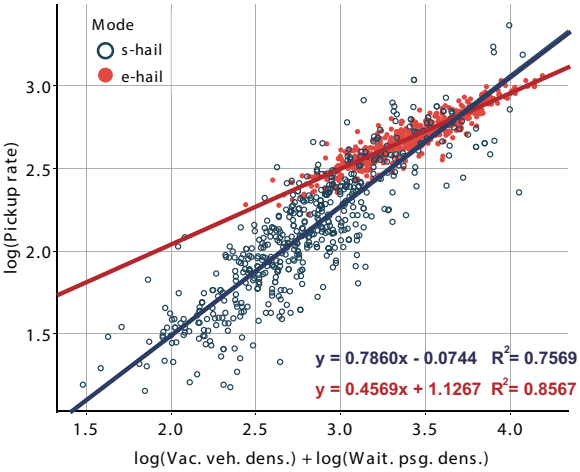

Figure 3: Empirical validation of ride-hail production functions. Each data point represents one local market at a given time period. The fitted linear equations are reported at the lower-right corner, along with their goodness-of-fit R^2. The intercept measures the logarithm of the total factor productivity (TFP), and the slope measures the output elasticity: $\log\hat{\beta}^s = -0.0744, \log\hat{\beta}^e = 1.1267, \hat{\alpha}^s = 0.7860, \hat{\alpha}^e = 0.4569$. Compared to s-hail, e-hail enhances TFP by 1489% ($\hat{\beta}^e/\hat{\beta}^s \simeq 15.89$) but lowers returns to scale by more than 40% ($\hat{\alpha}^e/\hat{\alpha}^s \simeq 0.58$), approaching constant returns to scale ($2\hat{\alpha}^e \simeq 0.9$). By contrast, s-hail displays increasing returns to scale ($2\hat{\alpha}^s \simeq 1.6$).

(*ii*) *Reachable Vehicle Fraction* (RVF, or $p(r)$) represents the fraction of vacant vehicles that are reachable by the passenger at a distance r from her.

With mild assumptions, we show the cumulative distribution function (CDF) of the passenger waiting time is,

$$F_{\tilde{w}}(t) = 1 - e^{-\int_0^t (2\pi\Lambda v^2/\delta^2) p(vt/\delta) t \mathrm{d}t}, \tag{2}$$

where v is the cruising speed of vacant vehicles and δ is a constant detour factor dependent on the topology of the road network. Based on Eq. (2), we may further specify the expected passenger waiting time for s-hail and e-hail separately.

First consider the case of s-hail, where passengers hail vacant vehicles off street (Figs. 4 (A) and (C)). Given the physical limit of eyesight, we expect EHD to be small ($d < 50m$), temporally stable, but sensitive to spatial localities of the market. In this case, RVF can be approximated by $p(r) = (\sigma d)/(2\pi r)$, where σ is a

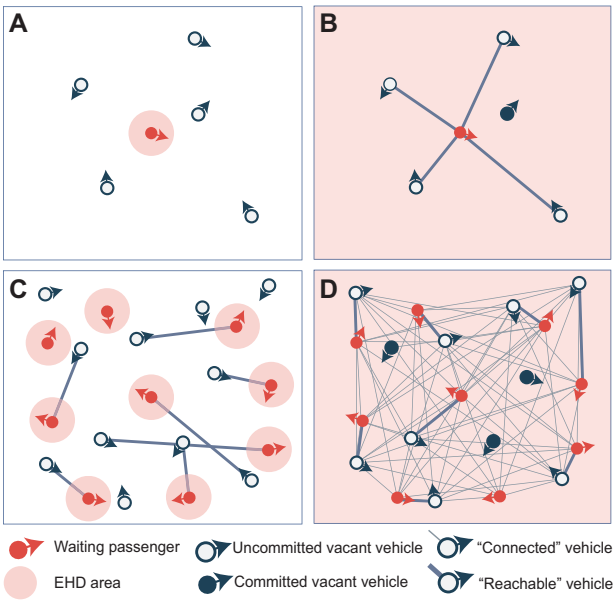

Figure 4: Illustration of passenger-driver matching mechanism. (**A**) In a low-density area, none of the five vacant vehicles around the s-hail passenger is reachable to her, due to her small EHD area. (**B**) In a low-density area, virtual connectivity enlarges the EHD area dramatically, making all four uncommitted vacant vehicles reachable to the e-hail passenger. (**C**) Higher density improves s-hail passengers' access to vacant vehicles. Only two out of nine passengers fail to find reachable vehicles. (**D**) In a high-density area, each of the nine e-hail passengers is connected to the same pool of eight uncommitted vacant vehicles. Yet, the competition leaves one passenger without any reachable vehicles.

correction factor that measures how attractive the passenger's waiting location is to nearby vacant taxis. Accordingly, the expected average waiting time for s-hail is

$$\bar{w}^s = \frac{\delta}{\sigma \Lambda d v}, \tag{3}$$

where d, σ, and v are calibrated for each local market (see [S3.1] in SI). Hence, ceteris paribus, $\bar{w}^s$ decreases quickly as more vacant vehicles (Λ) become available. This result is consistent with the observation in Fig. 2(A).

Unlike s-hail, e-hail can connect the passenger with vacant vehicles from afar (see Figs. 4(B) and (D)). Theoretically, this connectivity pushes EHD to infinity. However, the fact that many vacant vehicles are connected to the passenger does not mean they are all reachable. Instead, because other passengers now have equal access to the same pool of vacant vehicles, only a small fraction of the total supply will be allocated to the passenger as her reachable vehicles, presumably by certain matching algorithm. We hypothesize that RVF is approximated by $p = k/\Pi_0 \in (0, 1]$ (cf. Fig. 4(D)), where k measures the efficiency of the matching algorithm and Π_0 is the density of unmatched passengers (i.e., those who have placed orders but are waiting to be matched). Hence, the density of "reachable" vehicle is given by $k\Lambda_0/\Pi_0$ (Λ_0 is the uncommitted supply). This RVF leads to the expected waiting time for e-hail

$$\bar{w}^e = \frac{\delta}{2v}\sqrt{\frac{\Pi_0}{k\Lambda_0}} \simeq \frac{\delta}{2v}\sqrt{\frac{\Pi}{k\Lambda}}, \tag{4}$$

where k is calibrated from data for each local market (see [S3.2] in SI). Note that the expected passenger waiting time is inversely proportional only to the square root of the vehicle density ($\sqrt{\Lambda}$ or $\sqrt{\Lambda_0}$). In other words, AWT is less sensitive to uncommitted supply in e-hail than in s-hail, which can be seen by comparing Fig. 2(C) and (A).

To see how e-hail reduces the search friction, we derive the distributions of $\tilde{D} = \tilde{w}v$ for both services, where $\tilde{D}$ is the distance between the closest reachable vehicle and the passenger. We then compare $\lambda(r) = f(r)/[1 - F(r)]$, where $F(\cdot)$ is the CDF of $\tilde{D}$ and $f(\cdot) = F'(\cdot)$. Here $\lambda(r)$, often known as the hazard rate or failure rate in the literature, measures the rate of matching a reachable vehicle after searching for a distance r. It is easy to show s-hail has a constant $\lambda(r) = \sigma\Lambda d$, which is restricted by EHD. E-hail, however, enjoys a matching rate increasing with r, namely, $\lambda(r) = 2k\Lambda r/\Pi$. That is, e-hail is more likely than s-hail to find a reachable vehicle as the search radius expands. We attribute this advantage of e-hail to virtual connectivity, which reduces the *search friction*[14] through expanding the passenger's EHD area.

The ReV model also predicts that the competition among waiting passengers creates a congestion effect. The intensity of this effect may be measured by Π - the density of the waiting passengers - as the expected waiting time

for e-hail increases linearly with $\sqrt{\Pi}$. Therefore, accumulating a large number of waiting passengers in the system and allowing them to compete with each other eventually undermines the efficiency gained by the enhanced connectivity. We now explain how this congestion changes the relationship between AWT ($\bar{w}$) and the output (m), as revealed in Figs. 2(B) and (D). As per the Little's formula[15], at the stationary state, the effective passenger arrival rate within a unit area, denoted by q, equals the average number of waiting passengers divided by AWT, namely, $q = \Pi/\bar{w}$. The stationary condition also implies the pickup rate equals the arrival rate, that is, $m = q$. For s-hail, the Little's formula simply gives $\bar{w}^s \propto 1/m$, and for e-hail, it yields $\bar{w}^e \propto m$ by replacing Π in Eq. (4) with $m\bar{w}^e$. Thus, the prediction made by the ReV model well matches empirical observations in Figs. 2(B) and (D), supporting the explanation that the congestion induced by virtual connectivity eliminates the Mohring effect.

Furthermore, a relationship between the output m, the demand Π, and the supply Λ can be obtained for s-hail and e-hail, respectively, as

$$m^s = \frac{\sigma d v}{\delta}\Pi\Lambda; \quad m^e = \frac{2v\sqrt{k}}{\delta}\sqrt{\Pi\Lambda}. \qquad (5)$$

Eq. (5) also takes the form of the Cobb-Douglas function and can be compared against (1). According to the ReV model, s-hail has increasing returns to scale (with $2\alpha = 2$), whereas e-hail has constant returns to scale (with $2\alpha = 1$). This prediction matches well with the empirical observations in Fig. 3, which shows $2\alpha = 1.6$ for s-hail and 0.9 for e-hail. The model also suggests the TFP in e-hail is $2\sqrt{k}/(\sigma d)$ times of that in s-hail. We estimate $2\sqrt{k}/(\sigma d) \simeq 23.4$ with empirical results $d \simeq 0.036km, \sigma \simeq 1.5$ and $k \simeq 0.4$ (see [S3.3] in SI). Hence, e-hail is about 22 times more efficient than s-hail according to the ReV model. As a comparison, Fig. 3 shows an efficiency gain of about 15 times by e-hail, a reasonable agreement with the theory.

To summarize, the analysis above reveals two opposing forces at work. On the one hand, e-hail reduces the search friction by increasing the number of vacant vehicles that a passenger can reach. In low-density areas, this advantage helps dramatically improve the matching efficiency and lower the likelihood of unpleasantly long waits. On the other hand, virtual connectivity between passengers and drivers also leads to an unintended consequence. By enabling a large number of waiting passengers to compete for the same pool of vacant vehicles, virtual connectivity induces a *virtual congestion* effect that undercuts e-hail's returns to scale. This impact is most prominent in high-density areas, where e-hail apparently holds no clear advantage over s-hail.

What lessons could we learn from the findings above? First, simply scaling up may not help an e-hail operator become more efficient, because the industry displays near-constant returns to scale. This finding may be good news for small operators, because scale is hardly a barrier to entry. Second, limiting connectivity may be beneficial sometimes. For example, an e-hail operator could intentionally limit the matching radius to avoid excessive competitions among passengers, or simply price some out (known as surge pricing in practice[9]).

We close by noting that the unintended consequences created by virtual connectivity are ubiquitous. For example, social media can exacerbate perceived social isolation[16;17], even though it is invented to promote social connectivity. In e-commerce, virtual connectivity lowers the cost of searching for goods, but can increase consumer prices and reduce consumer welfare[18–22]. These negative impacts may be analyzed similarly as a matching problem. We hope that this work motivates others to examine this issue in other fields, and that the matching mechanism discovered herein finds applications beyond its domain.

Methods

Distribution of passenger waiting time

We aim to derive the distribution of passenger waiting time in a local ride-hail market. Consider the moment when a passenger arrives.

We define a *counting process* $\tilde{N}(r)$ as the number of vacant vehicles within a distance r from the passenger. Assume (*i*) all vacant vehicles are cruising at the same speed v, (*ii*) vacant vehicles are uniformly distributed with spatial density Λ, and (*iii*) the passenger keeps waiting at the same location until finally being picked up. Then, we prove that $\tilde{N}(r)$ is an *Inhomogeneous Poisson Process* with intensity function $\eta(r) = 2\pi\Lambda r$[23].

For each vacant vehicle at distance r from the passenger, RVF $p(r)$ determines the probability that the vehicle is reachable for the passenger, which is specified differently for s-hail and e-hail. Because the reachability of one vehicle is independent of that of others, $\tilde{N}(r)$ can be split into two independent sub-processes, corresponding to counting reachable and unreachable vehicles. Therefore, the number of reachable vehicles, denoted as $\tilde{N}_1(r)$, is also an Inhomogeneous Poisson Process with intensity function $\eta_1(r) = 2\pi\Lambda r p(r)$.

Suppose the passenger is picked up by the closest reachable vehicle, and denote $\tilde{D}$ as its distance to the passenger at the time when she enters the market. Then, the passenger waiting time $\tilde{w} = \delta\tilde{D}/v$, where δ is a constant detour factor that corrects the vehicle's travel distance prior to the pickup. Accordingly,

$$\begin{aligned} P(\tilde{w} \le t) &= P(\delta\tilde{D}/v \le t) = P(\tilde{D} \le vt/\delta) \\ &= 1 - P(\tilde{N}_1(vt/\delta) = 0) \\ &= 1 - \exp\left[-\int_0^{vt/\delta} \eta_1(r)\mathrm{d}r\right] \\ &= 1 - \exp\left[-\int_0^{t} \frac{2\pi\Lambda v^2 t}{\delta^2} p(vt/\delta)\mathrm{d}t\right]. \end{aligned} \tag{6}$$

Plugging in $p(r) = (\sigma d)/(2\pi r)$ for s-hail and $p(r) = k/\Pi_0$ (note that $\Pi_0/\Lambda_0 \simeq \Pi/\Lambda$) for e-hail, we finally derive the CDF of passenger waiting time in each service as

$$F_{\tilde{w}^s}(t) = 1 - \exp\left(-\frac{\sigma\Lambda d v}{\delta}t\right); \tag{7}$$

$$F_{\tilde{w}^e}(t) = 1 - \exp\left(-\frac{\pi k\Lambda v^2 t^2}{\delta^2\Pi}\right), \tag{8}$$

which yield the expected passenger waiting time in Eq. (3) and Eq. (4), respectively.

Model calibration

In this study, we calibrate s-hail and e-hail models in 277 local markets and two time periods for a week in 2016, which amounts to 1,108 models in total. Taxi GPS trajectory data is used for calibrating s-hail models. For e-hail, we use a random sample of trip records and cruising time of uncommitted vacant vehicles aggregated in each period and spatial units. Detailed descriptions of the local markets and data are provided in [S1] in SI.

Because the exact passenger waiting time of each pickup is not directly observed from the available data of s-hail, we develop a method to extract the maximum possible waiting time. We prove that, under mild conditions, the maximum possible waiting time follows the same distribution of passenger waiting time given the EHD value[23]. Using this important property, d and σ can be estimated using an iterative algorithm, provided that trajectories of all vacant vehicles are known[23]. In this study, we develop a calibration method based on incomplete trajectory data, as described in [S3.1] in SI.

A challenge in calibrating the e-hail model is to properly define the local market, based on which densities of waiting passengers and vacant vehicles are estimated. Although we focus on pickups in the core area, the passenger competition could exist in a much larger area. Additionally, the vacant-vehicle density consists of both uncommitted and committed vehicles. Hence, we need to transform the pickup distance into the committed-vacant-vehicle density Π_1. To this end, we first infer the supply area based on the distribution of pickup distance and then define a large area in which passengers may compete with each other (referred to as competing area). Based on the pickup location and the pickup distance, we compute the competing probability of each trip in the competing area, which may be interpreted as the likelihood of the passenger being counted in the local market of interest. Accordingly, the waiting-passenger density is estimated using the expected total waiting time within the com-

peting area, and the committed-vehicle density is estimated using the expected pickup distance within the supply area. More details about the calibration of the e-hail models are provided in [S2] and [S3.2] in SI.

Data Availability

The processed data that supports the findings of this study are available from the corresponding author upon reasonable request.

References

[1] Todd Litman. *Autonomous vehicle implementation predictions*. Victoria Transport Policy Institute, 2017.

[2] Tasha Keeney. The future of transport is autonomous mobility-as-a-service. *ARK Invest*, 2017.

[3] Judd Cramer and Alan B Krueger. Disruptive change in the taxi business: The case of uber. *American Economic Review*, 106(5):177–82, 2016.

[4] Eduardo M Azevedo and E Glen Weyl. Matching markets in the digital age. *Science*, 352(6289):1056–1057, 2016.

[5] George W Douglas. Price regulation and optimal service standards: The taxicab industry. *Journal of Transport Economics and Policy*, pages 116–127, 1972.

[6] Richard Arnott. Taxi travel should be subsidized. *Journal of Urban Economics*, 40(3):316–333, 1996.

[7] Hai Yang and SC Wong. A network model of urban taxi services. *Transportation Research Part B: Methodological*, 32(4):235–246, 1998.

[8] Liteng Zha, Yafeng Yin, and Hai Yang. Economic analysis of ride-sourcing markets. *Transportation Research Part C: Emerging Technologies*, 71:249–266, 2016.

[9] Juan Castillo, Daniel T Knoepfle, and E Glen Weyl. Surge pricing solves the wild goose chase. Available at SSRN: `https://ssrn.com/abstract=2890666`, 2018.

[10] Herbert Mohring. Optimization and scale economies in urban bus transportation. *The American Economic Review*, 62(4):591–604, 1972.

[11] William Vickrey. Optimal transit subsidy policy. *Transportation*, 9(4):389–409, 1980.

[12] Ian WH Parry and Kenneth A Small. Should urban transit subsidies be reduced? *American Economic Review*, 99(3):700–724, 2009.

[13] Charles W Cobb and Paul H Douglas. A theory of production. *American Economic Review*, 18:139–165, 1928.

[14] Ricardo Lagos. An alternative approach to search frictions. *Journal of Political Economy*, 108(5):851–873, 2000.

[15] John DC Little. A proof for the queuing formula: L= λ w. *Operations research*, 9(3):383–387, 1961.

[16] Junghyun Kim, Robert LaRose, and Wei Peng. Loneliness as the cause and the effect of problematic internet use: The relationship between internet use and psychological well-being. *CyberPsychology & Behavior*, 12(4):451–455, 2009.

[17] Sherry Turkle. *Alone together: Why we expect more from technology and less from each other*. Hachette UK, 2017.

[18] Jose Moraga-Gonzalez, Zsolt Sándor, and Matthijs Wildenbeest. Consumer search and prices in the automobile market, 2015. CEPR Discussion Paper No. DP10487. Available at SSRN: `https://ssrn.com/abstract=2579237`.

[19] José Luis Moraga-González, Zsolt Sándor, and Matthijs R Wildenbeest. Prices and heterogeneous search costs. *The RAND Journal of Economics*, 48(1):125–146, 2017.

[20] Yuxin Chen and Song Yao. Sequential search with refinement: Model and application with click-stream data. *Management Science*, 63(12):4345–4365, 2017.

[21] Michael Choi, Anovia Yifan Dai, and Kyungmin Kim. Consumer search and price competition. *Econometrica*, 86(4):1257–1281, 2018.

[22] Tiago Pires. Measuring the effects of search costs on equilibrium prices and profits. *International Journal of Industrial Organization*, 60:179–205, 2018.

[23] Hongyu Chen, Kenan Zhang, Yu Marco Nie, and Xiaobo Liu. A physical model of street ride-hail. Available at SSRN: `https://ssrn.com/abstract=3318557`, 2018.

Supplementary Information is available in the online version of the paper

Acknowledgments. This work is partially supported by the National Science Foundation under the award number PFI:BIC 1534138 and by National Science Foundation of China (NSFC) under the award number 71671147.

Author Contributions. L.X., J.G., X.L. collected the data; K.Z., H.C., S.Y., Y.N. analyzed the data; H.C., K.Z., Y.N. developed and calibrated the model. Y.N. supervised the project. All authors contributed to writing the manuscript.

Author Information. Correspondence and requests for materials should be addressed to Y.N. (ynie@northwestern.edu).

Supplementary Information for Virtual Connectivity is a Mixed Blessing for Ride-Hail

Kenan Zhang†[1], Hongyu Chen†[1], Song Yao[2], Linli Xu[2], Jiaoju Ge[3], Xiaobo Liu[4], and Yu (Marco) Nie *[1]

[1]Department of Civil and Environmental Engineering, Northwestern University, IL 60208
[2]Carlson School of Management, University of Minnesota, MN 55455
[3]Harbin Institute of Technology Shenzhen Graduate School, Shenzhen, China
[4]School of Transportation and Logistics, Southwest Jiaotong University, Chengdu, China

S1 Data Description

The data of both s-hail and e-hail services are collected in Shenzhen, China for a week in 2016. The s-hail data consists of GPS trajectories of all registered taxis in the city over the study period with an average inter-record interval of 20 seconds. Each GPS record contains information including taxi license ID, time stamp, coordinates, instantaneous speed and heading, and passenger occupancy status (0/1 variable). Using the procedure described in [1], trajectories are first segmented according to flips in the occupancy status, generating 250 to 300 thousands daily occupied trips. The e-hail data consists of a random sample of trip records and cruising time of uncommitted vacant vehicles aggregated in each time period and spatial unit. The trip records are randomly selected with a sample rate of 6%, producing about 45 thousand trips per day. Each trip record includes coordinates of the trip origin and destination, order placement time, driver arrival time, trip starting/ending time, pickup distance, etc.

S2 Local Ride-Hail Market

S2.1 Definition

A local market for a given ride-hail service is defined by the combination of a core area and a time period. However, the demand and supply in the local market are not necessarily confined by the physical boundary of the core area. Instead, they are defined differently for s-hail and e-hail, according to the operational characteristics of these services.

For s-hail, we consider the demand as all pickups in the core area, and for each pickup, we define a "supply area" centered at the pickup location. The size of the supply area is selected such that all reachable vehicles are covered (i.e., RVF diminishes to 0 at the boundary), thus it often goes beyond the core area. For simplicity, in this study we set the supply area to be a square

*Corresponding author, E-mail: y-nie@northwestern.edu.
†These authors contributed equally to the work.

centered at the pickup location with an area of about $1km^2$. The reader is referred to [2] for more details about supply area.

To define the supply area for e-hail, we first find the centroid of all pickup locations recorded inside the core area, and then, centering at that point, draw a circle with a radius equal to 90th percentile of all pickup distances (the green circle in Fig. E2[1]). Defining the demand is more complicated, because a passenger waiting in the core area may compete with those both inside and outside the supply area. For example, the passenger outside the supply area is competing with passengers in the study area as he/she may be closer to a vacant vehicle in the supply area (see Fig. E2(B)). Therefore, we need to consider waiting passengers in an even larger area, called the "competing area" (the orange circle in Fig. E2). The competing area is defined as a circle that is concentric with the supply area but doubles its radius. Accordingly, waiting passengers in the competing area who compete for vacant vehicles in the supply area contribute to the demand in this local market, which will be further specified in the following section.

S2.2 Aggregate measures

Given the definition of demand and supply, three aggregate measures are estimated in each local market, i.e., vacant vehicle density Λ, waiting passenger density Π and pickup rate m. For s-hail, the vacant vehicle density is estimated in the same way as described in [2], which is equivalent to the uncommitted supply, i.e., $\Lambda = \Lambda_0$. Waiting passenger density and pickup rate are given by

$$\Pi = \frac{1}{\mu HC} \sum_{i=1}^{N} t^i, \quad m = \frac{N}{\mu HC}, \tag{S1}$$

where H is the length of analysis time period, N is the number of pickups observed in the core area within H, μ is the sample rate (see S3 for more details), t^i is the passenger waiting time of ith pickup, and C is the core area. Since the exact passenger waiting time is not available from the s-hail data, multiple random draws are first taken based on the calibrated model. For each draw, we compute Π from Eq. (S1), then the sample average is used as the final estimate.

For e-hail, the uncommitted supply Λ_0 is directly obtained from data. Estimating committed supply Λ_1 and waiting passenger density, however, is more complicated and has to be addressed in the competing area. For each pickup observed in the competing area, we need to determine (1) the probability that the pickup is associated with the local market, denoted as p, and (2) when $p > 0$, how much it contributes to the committed supply, which is quantified by P_c, a fraction of its pickup distance.

Consider a pickup in the competing area. Let P be the pickup distance, L be the distance from the pickup location to the center of the market, and R be the radius of supply area. We specify p and P_c for the following two cases, each of which has three subcases (see Fig. E3).

1. The pickup is located inside the supply area, i.e., $L \leq R$.

   (a) $P \leq R - L$ (Fig. E3(A1)): In this subcase, the pickup vehicle must start inside the supply area. Hence, the passenger associated with the pickup is definitely part of the demand in the market and the entire pickup distance should be counted in the committed supply, i.e., $p = 1$ and $P_c = P$.

[1] All figures mentioned herein are presented in Extended Data.

(b) $P > R + L$ (Fig. E3(A2)): In this subcase, the pickup vehicle starts outside the supply area. Hence, the passenger did not compete for the supply inside the supply area of the market. Then pickup event has no contribution to either demand or supply. $p = 0$ and $P_c = 0$.

(c) $R - L < P \leq R + L$ (Fig. E3(A3)): In this subcase, the pickup may or may not start inside the supply area. The probability that it starts inside can be computed as $p = \theta_1/\pi$, where θ_1 can be solved by the law of cosine (i.e., $R^2 = L^2 + P^2 - 2LP\cos\theta_1$). Accordingly, the contribution of the pickup distance to the committed supply is $P_c = P\theta_1/\pi$.

2. The pickup is located outside the supply area, i.e., $L \leq R$.

(a) $P \leq L - R$ (Fig. E3(B1)): In this subcase, the pickup vehicle must start outside the supply area. As per the argument in 1(b), $p = 0$ and $P_c = 0$.

(b) $P > L + R$ (Fig. E3(B2)): $p = 0$ and $P_c = 0$ for the same reason as in 1(b).

(c) $L - R < P \leq L + R$ (Fig. E3(B3)): Similar to 1(c), the probability that the pickup vehicle starts inside the supply area is θ_1/π. However, only a fraction of the pickup distance is covered by the supply area. To be consistent with the estimate of committed supply, we count a cropped distance $P' = P - L\cos\theta + \sqrt{R^2 - (L\sin\theta)^2}$, and approximate the average of P' by

$$\begin{aligned}\bar{P}' &= \frac{1}{\pi}\int_0^{\theta_1}\left(P - L\cos\theta + \sqrt{R^2 - (L\sin\theta)^2}\right)\mathrm{d}\theta \\ &\approx \frac{\theta_1}{\pi}P - \frac{\sin\theta_1}{\pi}L + \frac{1}{\pi}\sqrt{\theta_1^2\left(R^2 - \frac{L^2}{2}\right) + \frac{\theta_1\sin 2\theta_1}{4}L^2}.\end{aligned} \tag{S2}$$

Hence, the contribution of the pickup distance to the committed supply is given by $P_c = \bar{P}'\theta_1/\pi$.

Given the specification of p and P_c for each pickup, the waiting passenger density and committed supply are finally estimated as

$$\Pi = \frac{1}{\mu H\pi R^2}\sum_{i=1}^{N^c} t^i p^i, \quad \Lambda_1 = \frac{1}{\mu H\pi R^2}\sum_{i=1}^{N^c} t^i \frac{P_c^i}{P^i}, \tag{S3}$$

where N^c is the number of pickups observed in the competing area.

Two different pickup rates are computed for e-hail. In Fig. 1 and Fig. 2 of the main text, pickup rates are computed in core areas so that the magnitude of the rates is comparable to that for s-hail, i.e. they are measured for exactly the same area. In Fig. 3, the pickup rates for e-hail are computed with respect to each local market, i.e.,

$$m^c = \frac{1}{\mu H\pi R^2}\sum_{i=1}^{N^c} p^i. \tag{S4}$$

This is necessary because here we aim to examine the production function of local markets. To that end, the output of the local market must include all pickups associated with it (not just those in its core area), as clarified in the above explanation.

S3 Model Calibration

Two time periods - a morning off-peak period (9 AM - 12 PM) and an evening peak period (5 PM - 8 PM) - and 277 core areas are selected for the model calibration. Thus, in total we calibrated the ReV model for 277×2 local markets for each service. Each core area corresponds to one or several traffic analysis zones (TAZ) defined by the city's urban planning agency, and is selected to have similar size and adequate ride-hail activities. Fig. E4 shows how these areas are distributed in the six municipal districts of the city, which are further categorized into three groups, i.e., downtown ("D"), urban ("U") and suburban ("S").

S3.1 Calibration of s-hail model

There are three main challenges in calibrating the ReV model for s-hail : (1) the exact passenger waiting time cannot be directly observed from the data; (2) two key parameters, i.e. d and σ, are entangled in the model thus cannot be estimated separately; and (3) due to various data collection issues, not all taxi trajectories are valid, hence the model calibration must be conducted with incomplete data. We briefly present our solution for the last one as the first two problems have been addressed in [2].

A critical step in the calibration is to construct the empirical mapping from each possible waiting time to the maximum possible EHD, i.e. $g : w \to d_M$. In short, we determine the upper bound of EHD by the distance from the pickup location to the pickup vehicle during its cruising phase (when it must not be engaged with the passenger) and to the closest other reachable vehicles, which requires trajectories of all vacant vehicles. In practice, however, we do not always have full access to the data or sometimes there are a considerable amount of errors in the data. Here we show the passenger maximum waiting time can still be properly estimated when trajectory data is incomplete.

Assume that: (1) observed and unobserved vacant vehicles are randomly and independently distributed in the supply area with density Λ_o and Λ_u, respectively; (2) all other parameters, i.e. v, d and σ, are the same among observed and unobserved vacant vehicles; and (3) the ratio between unobserved and observed vacant vehicles is known, denoted by μ. Following the same derivation as in [2], we can prove that the number of observed and unobserved reachable vehicles within a distance r from the passenger, denoted by $\tilde{N}_1^o$ and $\tilde{N}_1^e$, are Homogeneous Poisson Processes with intensity functions $\eta_1^o = \Lambda_o d$ and $\eta_1^u = \Lambda_u d$, respectively, Thanks to the independence, $\tilde{N}_1^o$ and $\tilde{N}_1^e$ merge into a Homogeneous Poisson Process $\tilde{N}_1$ with intensity $\eta_1 = (\Lambda_o + \Lambda_u)d = (1+\mu)\Lambda_o d$. Accordingly, the expected passenger waiting time is

$$E[\tilde{w}^s] = \frac{\delta}{\sigma v \Lambda d} = \frac{\delta}{\sigma v (1+\mu)\Lambda_o d}. \tag{S5}$$

The main difficulty lies in building the empirical mapping g, as we no longer observe the exact distance from the closest other reachable taxi to the pickup location. Given a possible waiting time w, we denote d_M^o and d_M^u as the distance from the closest observed and unobserved reachable taxi to the passenger, respectively. In essence, we need the maximum possible EHD as

$d_M = \min\{d_M^o, d_M^u\}$. Due to the missing data, we approximate d_M by taking its expectation

$$\begin{aligned} E[d_M] &= d_M^o P(d_M^o < d_M^u) + E[d_M^u | d_M^o \geq d_M^u] \\ &= \frac{1 - e^{-\sigma\Lambda_u d d_M^o}}{\sigma\Lambda_u d} = \frac{1 - e^{-\sigma\mu\Lambda_o d d_M^o}}{\sigma\mu\Lambda_o d}. \end{aligned} \tag{S6}$$

When d_M^o is very small, it is easily verified that $\sigma\mu\Lambda_o d d_M^o \to 0^+$. Hence, a Taylor expansion gives

$$E[d_M] = \frac{1 - \left[1 - \sigma\mu\Lambda_o d d_M^o + o\left((\sigma\mu\Lambda_o d d_M^o)^2\right)\right]}{\sigma\mu\Lambda_o d} \approx d_M^o. \tag{S7}$$

As d_M^o increases, $E[d_M]$ gradually deviates from d_M^o and approaches $E[d_M^u] = 1/(\sigma\Lambda_u d)$. Therefore, $E[d_M]$ is well bounded between d_M^0 and $1/(\sigma\Lambda_u d)$. Note that the gap between the lower and upper bounds grows as d, σ or μ increases, because there would be a larger probability mass for small realizations of d_M^u. Examples of observed and corresponding expected maximum EHD are illustrated in Fig. E5).

Since computing $E[d_M]$ requires d and σ, we develop an iterative calibration algorithm with two loops. The inner-loop performs the calibration procedure introduced in [2], while $\hat{d}$ and $\hat{\sigma}$, as well as the empirical mapping, are updated in the outer-loop. The initial estimates are generated without consideration of the missing data. $\hat{d}$ and $\hat{\sigma}$ are then updated by

$$\hat{d}_{out}^k = \hat{d}_{out}^{k-1} + \alpha(\hat{d}_{in}^{k-1} - \hat{d}_{out}^{k-1}), \tag{S8}$$

$$\hat{\sigma}_{out}^k = \hat{\sigma}_{out}^{k-1} + \alpha(\hat{\sigma}_{in}^{k-1} - \hat{\sigma}_{out}^{k-1}), \tag{S9}$$

where $\hat{(\cdot)}_{in}, \hat{(\cdot)}_{out}$ are estimates in the inner- and outer-loop, respectively, and α is a constant moving step (set to be 0.5 in this study).

S3.2 Calibration of e-hail model

In addition to Λ and Π described in S2, there are two parameters to be calibrated in the ReV model for e-hail, i.e., the cruising speed v and the matching parameter k. For simplicity, v is computed as the average pickup velocity of all pickups observed in the core area. Hence, the log-likelihood function of k is constructed as

$$\mathcal{L}(k) = \log \prod_{i=1}^{N} f_{\vec{w}}^e(t^i) = \sum_{i=1}^{N} \log \left\{ \frac{2\pi k \hat{\Lambda} \hat{v}^2 t^i}{\hat{\Pi}\delta^2} \exp\left[-\frac{\pi \hat{\Lambda} \hat{v}^2 (t^i)^2}{\hat{\Pi}\delta^2} \right] \right\}. \tag{S10}$$

where t^i is the observed passenger waiting time of the ith pickup.

Maximizing Eq. (S10) thus yields the maximum log-likelihood estimator for k as

$$\hat{k} = \frac{N\hat{\Pi}\delta^2}{\pi\hat{\Lambda}\hat{v}^2 \sum_{i=1}^{N} (t^i)^2}. \tag{S11}$$

S3.3 Main calibration results

Fig. E6 reports main calibration results. EHD estimates narrowly range between 30-45 meters, with a median of 36 meters across all local markets. LAA estimates range between 1 and 3, with a median of about 1.5. These findings well match the physical meaning of the two parameters in

the ReV model for s-hail. As for e-hail, estimated values for the matching efficiency parameter k vary significant across the markets, from as low as close to zero to as high as more than 3. However, no correlation with the waiting passenger density is noticed. The median of k is about 0.415. Fig. E7 compares the estimated and observed average passenger waiting times for the purpose of validation. It shows that e-hail models tend to have better goodness-of-fit, likely because the data used in their calibration is of higher quality (they are actual observations of passenger waiting time). As expected, a lower sample rate leads to worse goodness-of-fit (see Fig. E7(B)).

References

[1] Yu Marco Nie. How can the taxi industry survive the tide of ridesourcing? evidence from shenzhen, china. *Transportation Research Part C: Emerging Technologies*, 79:242–256, 2017.

[2] Hongyu Chen, Kenan Zhang, Yu Marco Nie, and Xiaobo Liu. A physical model of street ride-hail. Available at SSRN: `https://ssrn.com/abstract=3318557`, 2018.

Extended Data for
Virtual Connectivity is a Mixed Blessing for Ride-Hail

Kenan Zhang†[1], Hongyu Chen†[1], Song Yao[2], Linli Xu[2], Jiaoju Ge[3], Xiaobo Liu[4], and Yu (Marco) Nie *[1]

[1]Department of Civil and Environmental Engineering, Northwestern University, IL 60208
[2]Carlson School of Management, University of Minnesota, MN 55455
[3]Harbin Institute of Technology Shenzhen Graduate School, Shenzhen, China
[4]School of Transportation and Logistics, Southwest Jiaotong University, Chengdu, China

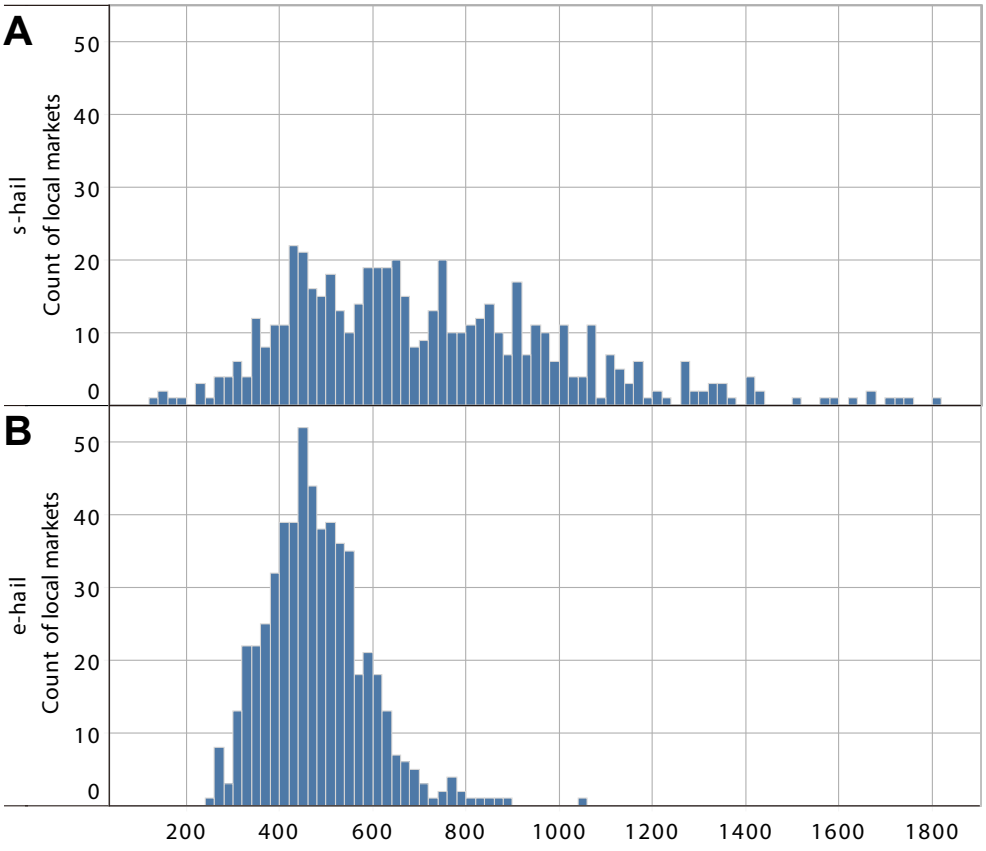

Figure E1: Histogram of 90-percentile passenger waiting time in each local market for (**A**) s-hail and (**B**) e-hail .

*Corresponding author, E-mail: y-nie@northwestern.edu.
†These authors contributed equally to the work.

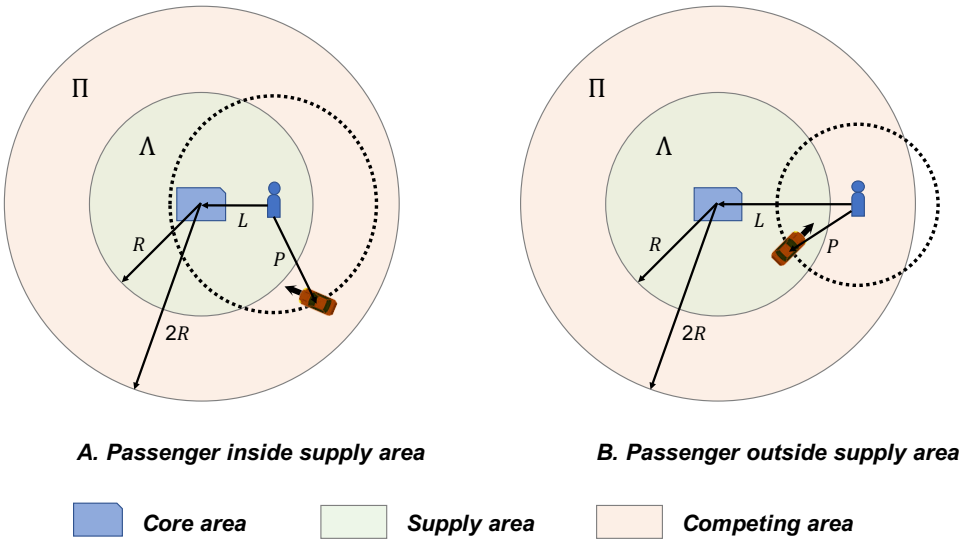

Figure E2: Illustration of the local market for e-hail.

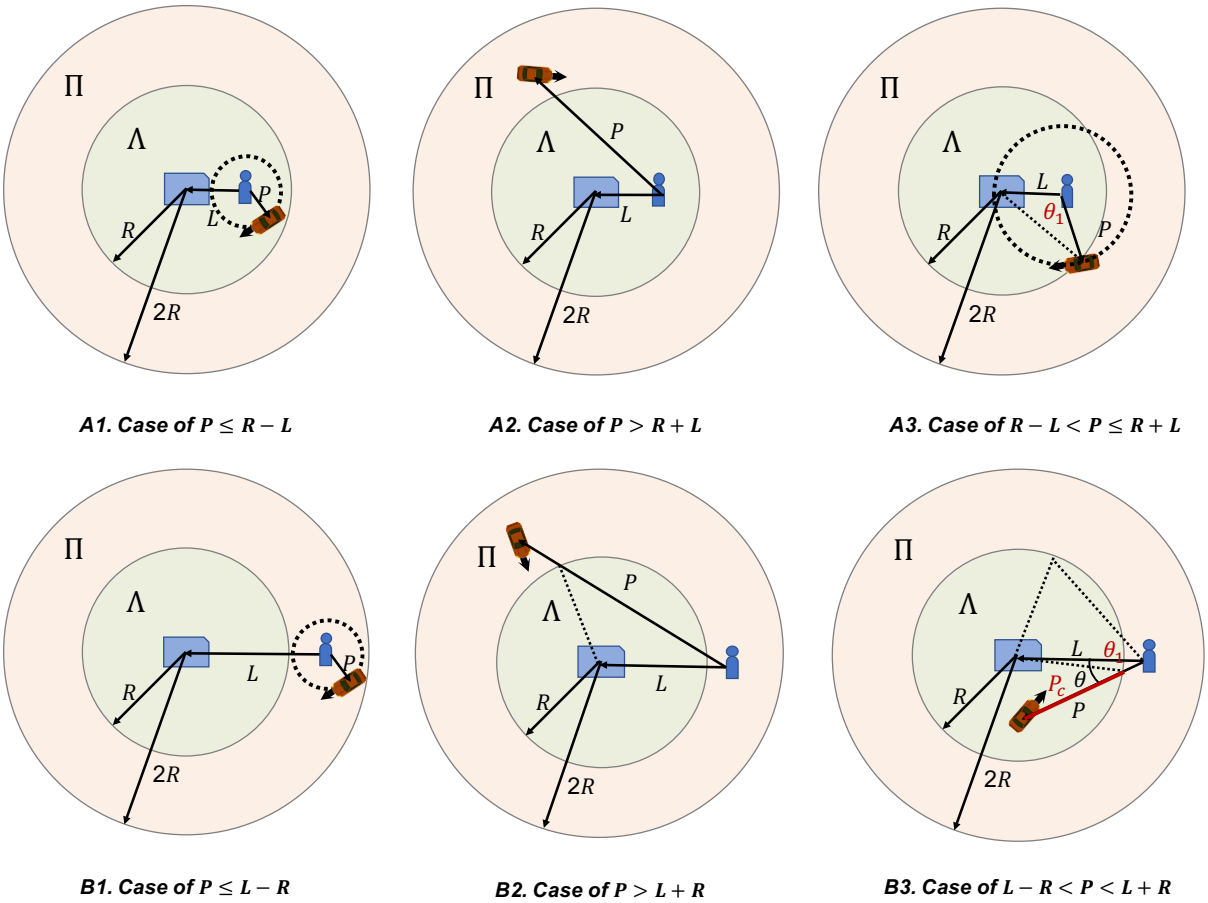

Figure E3: Six different cases considered for estimating the contribution of a pickup event in the competing area to a local market.

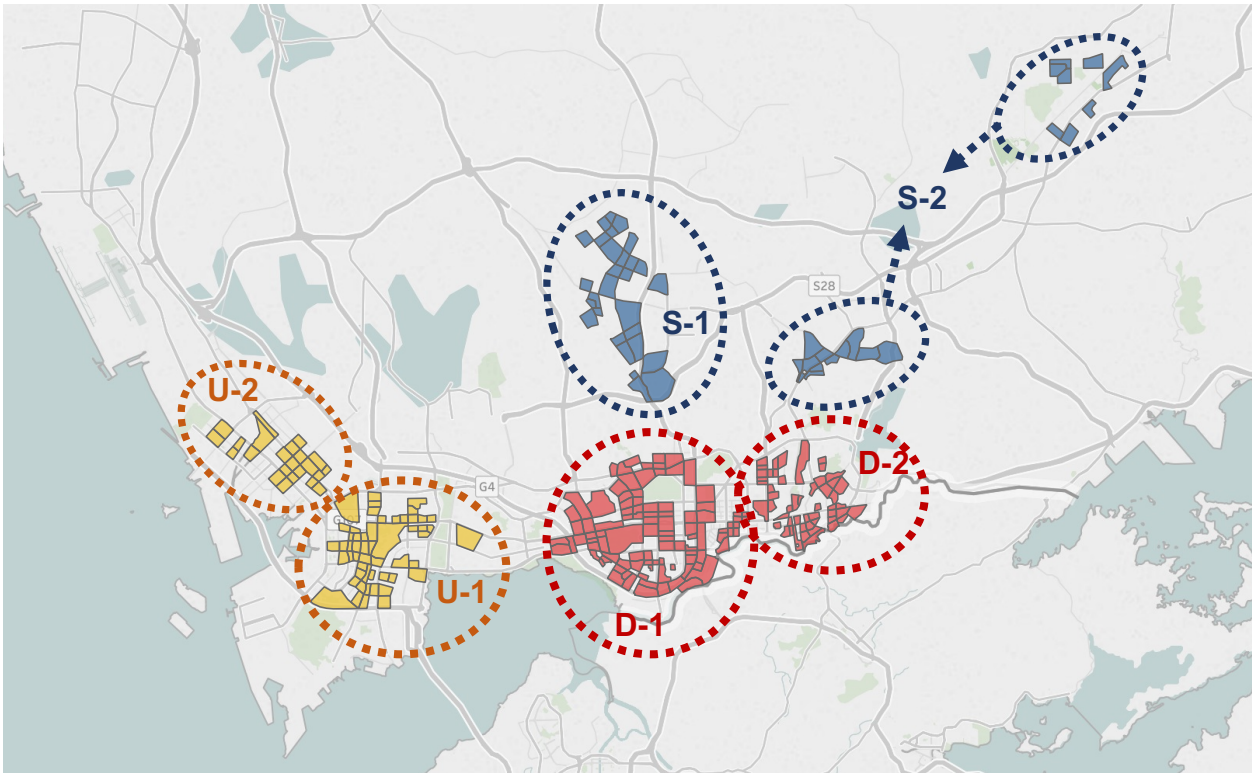

Figure E4: Distribution of 277 local markets in six municipal districts of Shenzhen.

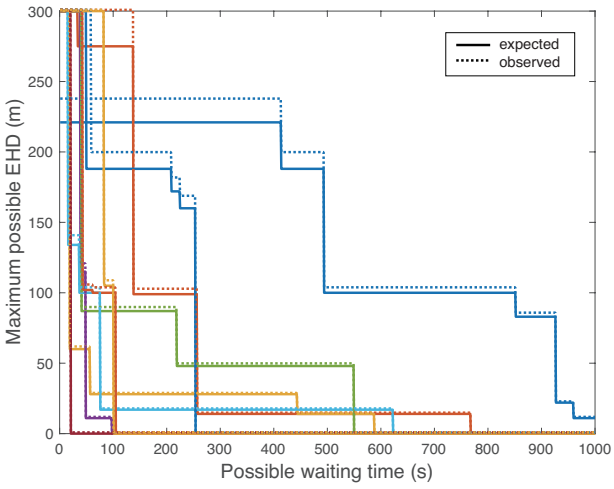

Figure E5: Sample empirical mappings with and without consideration of missing data. The other parameters are $\Lambda = 46.93/km^2$, $v = 2.5m/s$, $\mu = 0.8315$, $d = 15m$ and $\sigma = 1.0$.

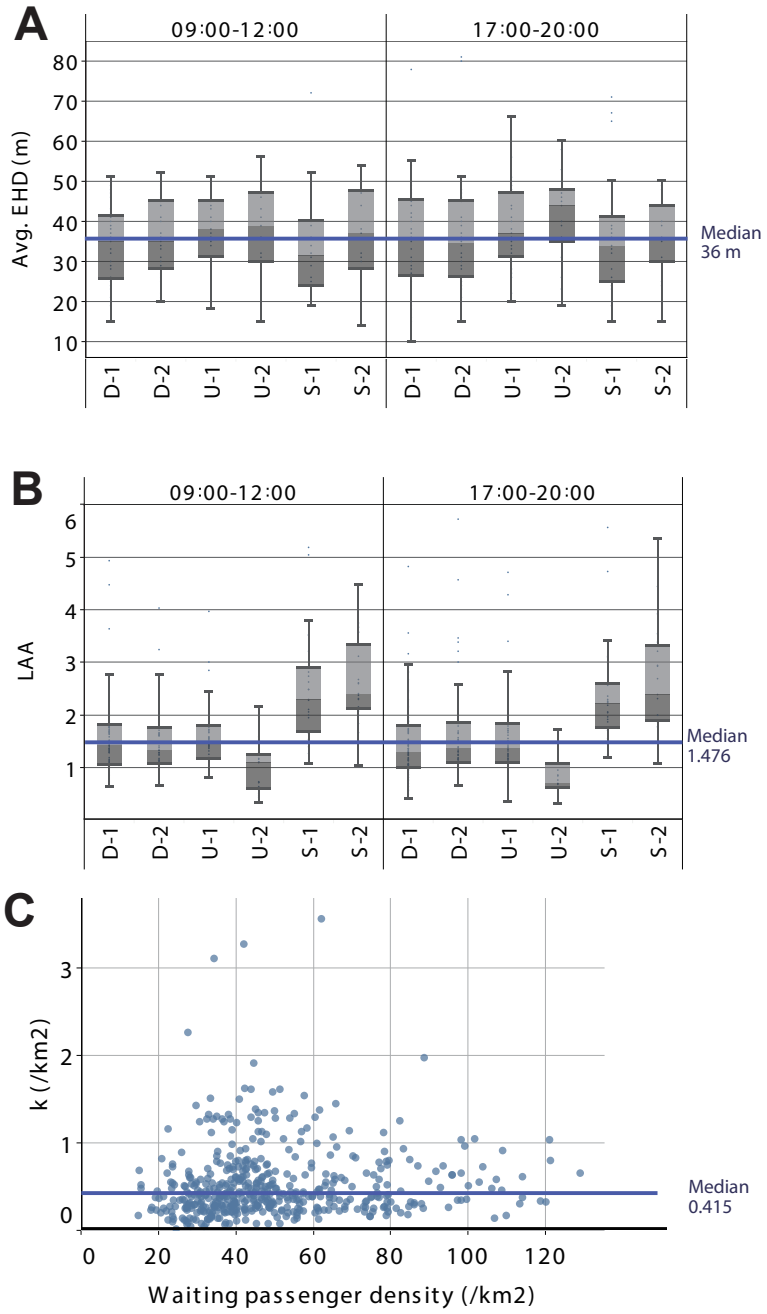

Figure E6: Main results of model calibration. (**A**) Boxplots of EHD estimates by municipal district and time period. (**B**) Boxplots of LAA estimates by municipal district and time period. (**C**) Estimates of k against waiting passenger density. The median estimate values over all local markets are also illustrated in each subplot.

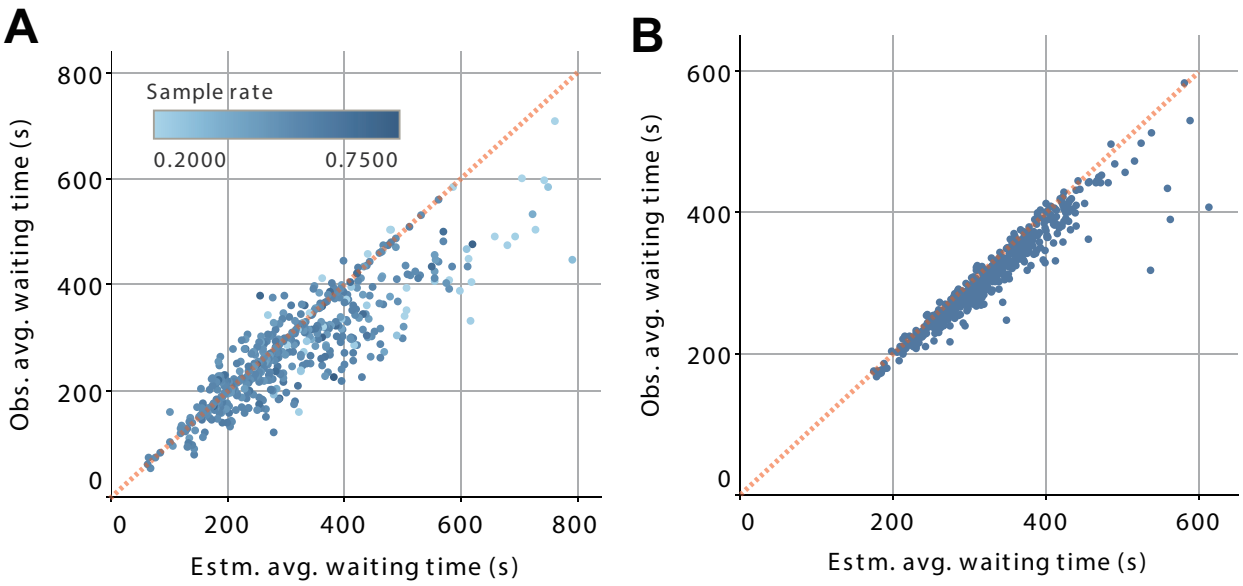

Figure E7: Simple validation of estimated average passenger waiting time for (**A**) s-hail and (**B**) e-hail. Points on the diagnoal dash line mean the model make correct predictions. The color of each point represents the sample rate.